

Dispersive atom interferometry phase shifts due to atom-surface interactions

S. LEPOUTRE¹, H. JELASSI¹, V. P. A. LONI², G. TRÉNEC¹, M. BÜCHNER¹, A. D. CRONIN² and J. VIGUÉ^{1(a)}

¹ *Laboratoire Collisions Agrégats Réactivité IRSAMC; Université de Toulouse-UPS and CNRS UMR 5589 F-31062 Toulouse, France, EU*

² *Department of Physics, University of Arizona - Tucson, AZ 85721, USA*

received 25 June 2009; accepted in final form 1 October 2009

published online 28 October 2009

PACS 03.75.Dg – Atom and neutron interferometry

PACS 34.50.-s – Scattering of atoms and molecules

PACS 34.20.-b – Interatomic and intermolecular potentials and forces, potential energy surfaces for collisions

Abstract – We used the Toulouse atom interferometer to study how Van der Waals (VdW) interactions between atoms and surfaces cause velocity-dependent phase shifts for atomic de Broglie waves. By introducing a thin nano-grating in one branch of this interferometer, we observed a phase shift that depends on velocity to the power -0.49 . This dispersion serves to measure both the strength and the position dependence of the atom-surface potential in the range from 5 to 10 nm from the surface, and it can also set new limits on non-Newtonian gravity in the 2 nm range.

Copyright © EPLA, 2009

Atom interferometers are celebrated tools for measuring atomic de Broglie wave phase shifts [1]. By transmitting one arm of an atom interferometer through a nano-structure, an electric field, or a dilute gas, measurements have been made of Van der Waals (VdW) potentials [2] atomic polarizabilities [3–5], and complex scattering amplitudes [6–8] respectively. Studies of *dispersion*, *i.e.* phase shifts as a function of atomic velocity, provide additional information about the interactions that cause these phase shifts. For example, glory undulations observed in [7,8] can reveal the number of bound states in atom-atom potentials as well as the long-range shape of such potentials. Here, we report the first observations of dispersive phase shifts caused by atom-surface interactions with enough precision to measure both the strength and the position dependence of the atom-surface potential.

Atom-surface interactions in the non-retarded Van der Waals regime and in the longer-range Casimir-Polder regime [9] are the topic for hundreds of references in the field of QED [10]. These interactions are important for a large variety of experiments involving atoms or molecules near surfaces: atoms or molecules passing through nano-gratings [11–13]; propagation of molecules in Talbot-Lau interferometers using material gratings [14]; reflection properties of atomic mirrors using evanescent

laser waves [15–17] including atom interferometry experiments [18,19]. Atom-surface interactions are necessary to understand quantum reflection from nano- or micro-structured surfaces [20–23], BEC interferometry on a chip [24], MOT dynamics near an optical fiber [25,26], or searches for nanometer-scale modifications to Newtonian gravity [27].

The first measurement of atom-surface interactions by atom optics techniques was made by the research group of J. P. Toennies in 1999 [11], by measuring the intensities of the various diffraction orders transmitted by a nano-grating and this work was followed by similar experiments [28,29]. Atom interferometry can be used to measure the phase shift associated to diffraction by a nano-grating, as first done by the research group of one of us (ADC) [2,30]. The long-range part of this potential has been studied by observing quantum reflection of atoms [31]. Laser spectroscopy, which can be also used to study atoms near surfaces [32], is sensitive only to the difference of the interaction potentials corresponding to the atom internal states connected by the laser. We cannot review here all the other methods available to study the atom-surface interaction potential and we refer the reader to the review paper by Hoinkes [33].

Deviations from the C_3/r^3 form of the atom-surface potential can be caused by retardation, adsorbed atoms, and in principle by gravity [34]. There is therefore

^(a)E-mail: jacques.vigue@irsamc.ups-tlse.fr

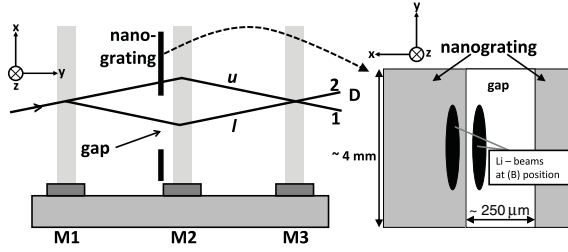


Fig. 1: Left part: experimental set-up of our interferometer. A supersonic beam of lithium is diffracted by three standing laser waves, forming a Mach-Zehnder atom interferometer. The laser standing waves are obtained by reflecting three lasers beams on the mirrors noted M_i with $i = 1-3$. A nano-grating can be inserted just before the second standing wave, at the position where the distance between the two atomic beams labelled u and l is largest, of the order of $100 \mu\text{m}$. The output beams labelled 1 and 2 carry complementary fringe signals and the detector D measures the intensity of one of these two beams. Right part: schematic drawing of the nano-grating showing the $250 \mu\text{m}$ wide gap and the atomic beams with the “ u ” beam going through the grating and the “ l ” beam going through the gap.

motivation to measure the strength and functional form of the atom-surface interaction potential with unprecedented accuracy. The methods and analysis presented here advance the Atom Optics techniques available for such measurements.

We use a silicon nitride nano-structure with 53 nm wide windows as a phase shifter in an atom interferometer. With lithium atom beams with velocity v in the range 700 to 3400 m/s , our measurements show a surface-induced phase proportional to $v^{-0.49}$. This is contrary to the naive prediction of v^{-1} , therefore we are motivated to present an analytical model to explain this unusual dispersion and discuss its implications for new applications for atom interferometry.

We emphasize that the first experiment [2] to detect surface-induced phase shifts with an atom interferometer was not accurate enough to study dispersion, and therefore could not test the power law of the potential. By comparison, the measurements presented here have a 30 times improved accuracy for phase shifts at any one velocity. In this manuscript, we explain the improved methods and observations first. Then we discuss the origin of the dispersion. Finally, we discuss the significance of this dispersion for new measurements, such as searches for non-Newtonian gravitational interactions.

Our experiment uses the Toulouse atom interferometer discussed in [35]. The experimental set-up is shown on fig. 1. A supersonic beam of lithium atoms seeded in a carrier gas crosses three near-resonant laser standing waves that diffract the beam, thus forming a Mach-Zehnder atom interferometer. This atomic beam is highly collimated by two slits with widths ca. $15 \mu\text{m}$ (the exact value depending on the carrier gas used for the supersonic expansion) separated by 0.76 m , resulting in an atomic

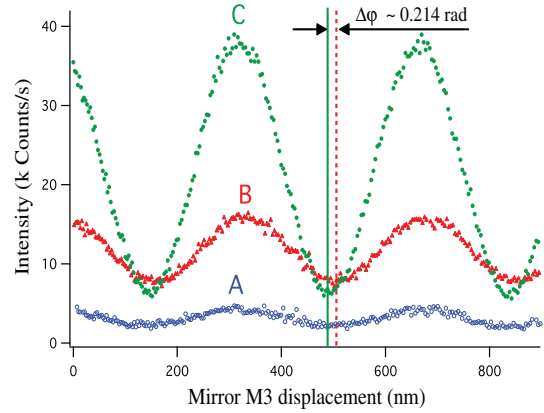


Fig. 2: (Colour on-line) Atom interference fringes recorded with (A) both arms (visibility $\mathcal{V}_A = 32\%$), (B) one arm ($\mathcal{V}_B = 34\%$), or (C) neither arm ($\mathcal{V}_C = 72\%$) passing through the nano-structure, with a lithium beam velocity $v = 1062 \pm 20 \text{ m/s}$. The counting period is 0.1 s per data point.

beam angular width close to $20 \mu\text{rad}$ FWHM. This high collimation is needed to separate the u and l beams in the interferometer and also the two output beams labelled 1 and 2 in fig. 1. Because the light gratings match the Bragg condition, the Toulouse interferometer has only two arms, as opposed to the interferometer used in [2]. The results are dramatically easier to interpret so we were able to measure the surface-induced phase shift with an uncertainty of 2%.

The measured intensity output from the interferometer depends on the positions x_i of the three standing-wave mirrors M_i [35] and a phase φ :

$$I = I_0 [1 + \mathcal{V} \cos(k_g(x_1 - 2x_2 + x_3) + \varphi)]. \quad (1)$$

Here, I_0 is the mean intensity, \mathcal{V} is the fringe visibility, and k_g is the light-grating k -vector. To observe atom-interference fringes, shown in fig. 2, we displace mirror M_3 with a piezo drive. We measure its position using a Michelson interferometer involving M_3 and a fixed mirror. This interferometer is completely under vacuum and operated with a He-Ne laser. The resulting uncertainty on measurements of the phase φ of the atom interference fringes is about 3 milliradians, for a 100 second recording with neither arm going through the nano-grating, as in recording C of fig. 2.

We locate the phase-shifting nano-structure just before the second laser standing wave. The distance between the two interferometer arms, which is largest at this point, is inversely proportional to the atom velocity v and close to $100 \mu\text{m}$ when $v = 1000 \text{ m/s}$ with first order Bragg diffraction. For velocities larger than 2000 m/s , we use second order Bragg diffraction to increase the path separation. However, in this case, the interference fringes have a lower visibility and some stray beams due to weak first order diffraction are present. These two defects

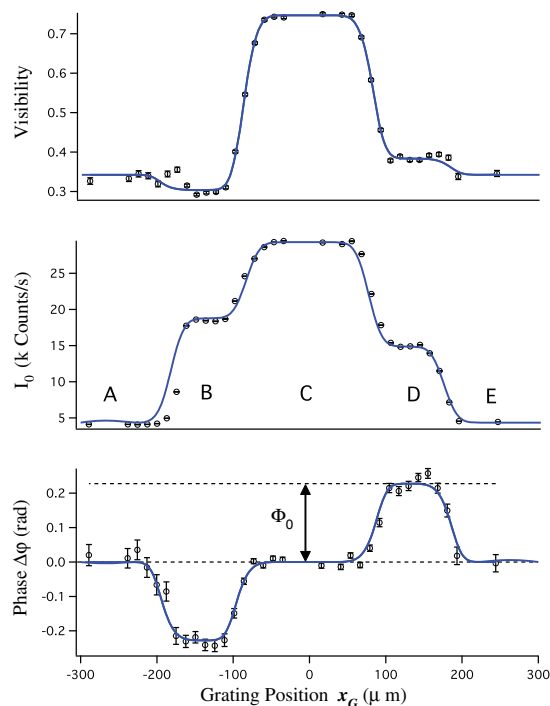


Fig. 3: (Colour on-line) Measured fringe visibility \mathcal{V} , mean intensity I_0 , and phase shift $\Delta\varphi$ shown as a function of the interaction grating position x_G , for a lithium beam velocity $v = 1062 \pm 20$ m/s. At the reference position, $x_G = 0$, both interferometer arms go through the gap, so they are unaffected by the grating. When $65 < |x_G| < 190 \mu\text{m}$ (case B or D), only one arm goes through the grating and we observe opposite phase shifts. The mean intensity and the fringe visibility are reduced, as discussed in the text. When $|x_G| > 190 \mu\text{m}$ (case A or E), both arms go through the grating, the phase shift returns to 0. The best fit is represented by the continuous line.

reduce the accuracy of our phase measurements when $v > 2000$ m/s.

Our phase-shifting element is the same interaction grating used in the Perreault experiment [2], except that the gap for the reference beam has been enlarged from 100 to $250 \mu\text{m}$ and the structure has been sputter-coated with Au/Pd metal. The enlarged gap makes data shown in fig. 3 much easier to interpret. The thin (nominally 1 nm thick) layer of Au/Pd made the structure more suitable for SEM imaging, and may have increased the C_3 VdW coefficient. This free-standing, Au/Pd-coated, silicon nitride membrane has an array of 53 ± 1 nm wide windows that are regularly spaced, with a period of $d_G = 100 \pm 0.1$ nm: the width to period ratio has been very accurately measured by atom diffraction studies [36]. Atoms transmitted through these windows must therefore have passed within 26.5 nm of a material surface. This causes the VdW-induced phase Φ_0 . The interaction grating is on a translation stage so that either one (or both) of the interferometer arms can pass through the gap, relatively far

from any surfaces. Hence, the interference fringes can shift in phase by as much as $\Delta\varphi = \pm\Phi_0$, with the sign depending on which arm goes through the interaction grating.

The windows are oriented horizontally such that diffraction from the periodic structure deflects atoms out of the plane of the interferometer. Beam components that are diffracted by the nano-grating no longer match the Bragg condition of the light gratings, and thus contribute only incoherent background flux. Only the direct, 0th order, beam contributes to the interference signal and we note A_0 the transmission amplitude of this order. The observed phase shift $\Delta\varphi$ is equal to $\pm\Phi_0$ where Φ_0 is the argument of the complex amplitude A_0 . A_0 has a modulus less than 1 and only $|A_0|^2 \sim 8\%$ of the incident flux is transmitted into the 0th order. As a consequence, the fringe intensity and visibility are both reduced when one arm goes through the interaction grating. Moreover, these reductions are not the same when one arm goes through the nano-grating as compared to the other arm. This is because, initially, the interferometer is slightly unbalanced, with more de Broglie wave amplitude in one arm. When both atomic arms go through the nano-structure, the measured phase is expected to be the same as when both arms go through the gap, but the intensity and visibility are modified. A complete description of the signal as the interaction grating translates across both interferometer arms is beyond the scope of the present letter, and will be presented elsewhere. Results from this experiment and a best-fit model are shown in fig. 3. Five conditions are identified, with the interaction grating attenuating (A) both arms, (B) one arm, (C) neither arm, (D) the other arm, and (E) both arms again. The cases B and D provide two measurements of the grating phase shift, Φ_0 , corresponding to different parts of the interaction grating. These two measurements are in good agreement, as a consequence of the good homogeneity of the grating.

The visibility, mean intensity, phase shift profiles in fig. 3 are significantly different than in the Perreault experiment [2], for which profiles are published in [37]. The larger gap and better resolved interferometer arms help to make clear plateaus in fig. 3. The presence of only two arms due to Bragg diffraction also helps to make the profiles in fig. 3 much easier to model. After these improvements, the dominant source of uncertainty in our determination of Φ_0 is phase drift. We compensate for phase drift by making alternate measurements, a reference scan allowing both interferometer arms to pass through the grating gap and a measurement scan with the grating at a different position. The phase shift $\Delta\varphi$ is taken as the phase difference between the measurement scan and the mean of the two reference scans done just before and just after the measurement. In this way, an individual measurement of the phase shift $\Delta\varphi$ has a statistical uncertainty $\sigma \approx 20$ mrad. During a run of few hours, we can get several tens of such phase measurements thus providing a complete picture of the effect of the grating on the interferometer signals.

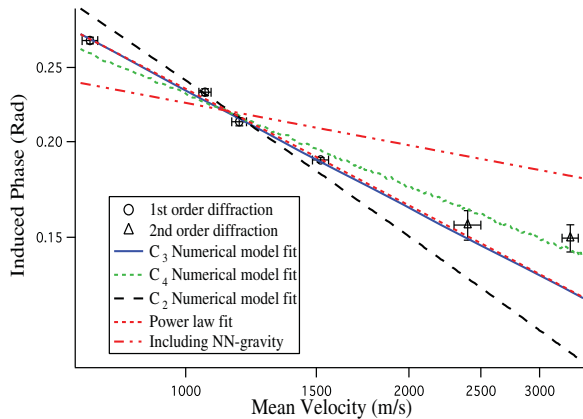


Fig. 4: (Colour on-line) Induced phase *vs.* beam velocity *v*. The experimental data points have been fitted by various models. The full line is a numerical model with the only free parameter being the C_3 coefficient, with a fitted value $C_3 = 3.25 \text{ meV} \cdot \text{nm}^3$. The power law fit which follows a $v^{-0.49}$ -dependence is represented by a dotted curve which is almost indistinguishable from the numerical fit. The numerical model has also been fitted assuming a $C_2 r^{-2}$ and a $C_4 r^{-4}$ atom-surface potential and these fits are very different: the dispersion of the phase shift with atom velocity appears to be very sensitive to the shape of the atom-surface potential. Finally, we have calculated the phase shift with our numerical model by adding to the VdW term (with a reduced C_3 value, $C_3 = 1.5 \text{ meV} \cdot \text{nm}^3$) a non-Newtonian gravity term with $\alpha = 10^{27}$ and $\lambda = 2 \text{ nm}$: in this case too, the dispersion is very different from the experimental results.

We collected similar data for six different velocities of the lithium beam covering the 700–3400 m/s range. The beam velocity was controlled by changing the carrier gas, and the velocity was measured by studying Bragg diffraction rocking curves and by Doppler-sensitive laser-induced fluorescence spectra. The experimental spread in velocity was typically 20% (FWHM) of the mean velocity.

To determine Φ_0 for each velocity, we have taken a weighted average of all the available measurements, with a weight inversely proportional to the square of their statistical uncertainty. The results are plotted as a function of the beam’s mean velocity v in fig. 4, and are well described by $\Phi_0 \propto v^{-0.49}$. The data point corresponding to $v = 3300 \text{ m/s}$ was not included in the fit, because it deviates from the general trend. We explain this deviation by the experimental problems associated with imperfect second order Bragg diffraction at that velocity.

Next, we discuss the origin of the phase shift and its dispersion. If the phase shift Φ_0 is from VdW interactions in the non-retarded regime, the potential is expected to be:

$$V_{\text{VdW}}(r) = -\frac{C_3}{r^3} \quad (2)$$

in the case of an infinite plane, r being the shortest distance to the surface and C_3 the VdW coefficient. We

approximate the potential for an atom in the window between two grating bars by the potential caused by two infinite planes coincident with the two nearest grating walls, as given in equation (2) and we then allow the potential to be “on” only while the atom is between the grating bars (for a detailed discussion, see [11,29]). The thickness of the grating can be modelled as a thin phase and amplitude mask. The grating bars have a trapezoidal cross section and we take the wedge angle α_G of the trapezoid into account when explaining the induced phase. Once the grating geometry is known in terms of the period d_G , window width w_G , thickness L_G and wedge angle α_G , the phase due to the interaction of the atom with the two nearest walls can be calculated in the WKB approximation:

$$\phi(x) = -\frac{1}{\hbar v} \int_0^{L_G} V_{\text{VdW}}(z, x; w_G, \alpha_G) dz. \quad (3)$$

Here $\phi(x)$ is the phase shift acquired by the incident wave just after the grating; this phase depends on the nanometer-scale position, x , within the grating windows. This position-dependent phase is inversely proportional to the velocity v . From $\phi(x)$, we deduce the complex amplitude A_n of the n -th diffraction order:

$$|A_n| e^{i\Phi_n} = \frac{1}{d} \int_{-w/2}^{w/2} \exp \left[i \left(\phi(x) - \frac{2\pi n x}{d} \right) \right] dx. \quad (4)$$

Our experiment measures the phase Φ_0 of the 0th order amplitude, which is given by:

$$\Phi_0 = \arctan \left(\frac{\int_{-w/2}^{w/2} \sin[\phi(x)] dx}{\int_{-w/2}^{w/2} \cos[\phi(x)] dx} \right). \quad (5)$$

In order to fit the Φ_0 data, we used a numerical model which takes into account the grating geometry. Even though this numerical model fits the Φ_0 data very well, it is interesting to explain by a simple analytic expression the dependence of this phase on the velocity. Cronin *et al.* have previously introduced a generalized Cornu spiral to visualize the integral in eq. (4) and to discuss the intensity $|A_n|^2$ of the various diffraction orders [38]. We have used the same analysis to develop an analytical expression for the phase Φ_0 . From a plot of the Cornu spiral (not shown here), the dominant contribution to Φ_0 comes from the region where $|\phi(x)| < \pi/2$; the contribution of the region with $|\phi(x)| > \pi/2$ is almost negligible since this is a region of rapidly oscillating phase.

To get an analytic expression of the phase shift Φ_0 , we must simplify eq. (4) and an obvious simplification is to note that, as $\phi(x)$ is an even function of x , we may take the integral only from $x=0$ to $x=w/2$ and double the result to get the amplitude A_0 . We may then assume that the phase $\phi(x)$ is only due to the nearest wall because, as shown by numerical calculations, the

dominant contributions to the amplitude phase Φ_0 are due to trajectories close to the wall (another way of explaining this approximation is to note that the exact value of $\phi(0)$ is considerably smaller than the value of Φ_0). We also assume that the wall is parallel to the atomic velocity (*i.e.* the wedge angle α_G is equal to 0). For positive x , the phase $\phi(x)$ is then given by

$$\phi(x) = \frac{C_3 L_G}{\hbar v [(w_G/2) - x]^3} \quad (6)$$

and, after a change of variables, Φ_0 is approximately

$$\Phi_0 \approx \frac{\int_{A^3}^{\infty} \sin[\phi] \phi^{-4/3} d\phi}{\int_{A^3}^{\infty} \cos[\phi] \phi^{-4/3} d\phi}. \quad (7)$$

Here $A^3 = \phi(0) = \frac{C_3 L_G}{\hbar v} (w/2)^{-3}$ is the phase acquired along the center of the window. We can expand both the numerator and the denominator in this expression in terms of A and find:

$$\Phi_0 \approx \frac{\Gamma(\frac{2}{3}) A}{2 - \sqrt{3} \times \Gamma(\frac{2}{3}) A} \approx \frac{1.35 (\frac{C_3 L_G}{\hbar v})^{1/3}}{w - 2.35 (\frac{C_3 L_G}{\hbar v})^{1/3}}, \quad (8)$$

where we have given only the first-order terms in A . An interesting point is that the dominant contribution to the integral of $\sin[\phi(x)]$ comes not from the center of the opening, where the atom-surface distance x is close to $w/2$, but from the region where $\phi(x) \approx 1$ rad, corresponding to an atom-wall distance $r_1 = [C_3 L_G / (\hbar v)]^{1/3}$. In our experiment, r_1 decreases from $r_1 \approx 9$ nm when $v = 700$ m/s to $r_1 \approx 5.6$ nm when $v = 3300$ m/s.

By taking the logarithmic derivative of eq. (8), we can deduce the exponent q of the best approximation of $\Phi_0(v)$ by a power law of the form $\Phi_0 \propto v^q$. We thus get $q = -\frac{w}{3(w - 2.35r_1)} \approx -0.48$ when $r_1 \approx 7$ nm, corresponding to a velocity $v \approx 1600$ m/s. This agrees well with our experimental data, but it is an unusual velocity dependence for a phase shift in atom optics. A uniform potential applied to one arm of an atom interferometer usually results in a phase proportional to v^{-1} . The velocity dependence is related to the spatial dependence of the potential. For example, a gas cell in one arm induces a phase proportional to $v^{-7/5}$ compounded with glory oscillations due to bound states. Topological phases, such as the Aharonov-Casher phase, are independent of velocity.

We explain the observed velocity dependence by the fact that the phase comes mostly from a region of distance to the wall which itself depends on velocity. The similarity to $q = -1/2$ is a coincidence. Equation (8) predicts $\Phi_0 \propto v^{[-1/p + f(v)]}$ where $f(v)$ is a velocity-dependent correction factor and p describes a more general ansatz for an atom-surface interaction potential given by $V = -C_p r^{-p}$.

In fact, using the numerical model and assuming an atom-surface interaction potential given by $-C_p/r^p$, we find that the best fit is obtained for $p = 2.9 \pm 0.2$. At any one velocity, we could not constrain the value of p . It is

the observed dispersion that provides sensitivity to p at short atom-surface separations.

The presence of non-Newtonian gravitational interactions can also be hypothesized as an explanation for the observed phase shifts. We analyzed our data using a model that includes a potential term $V_G(\ell) = -Gm_1m_2(1 + \alpha e^{-\ell/\lambda})/\ell$ with ℓ the distance to any volume element of the nano-structure. When we analyze the observed phase shifts with this potential we can constrain $(\alpha, \lambda) = (< 10^{26}, 2 \text{ nm})$ or $(\alpha, \lambda) = (< 10^{23}, 10 \text{ nm})$. At $\lambda = 2$ nm, this upper limit on α is comparable to previous upper limits [27,39]. We emphasize that the observed dispersion helps to set a more strict limit on α . In the future, α can be constrained by two additional orders of magnitude by using heavier atoms with a weaker atom-surface interaction such as xenon.

The analysis leading to eq. (8) also serves to make a prediction for much larger nano-structures, such as the ones described in [40]. For these structures with $w \gg r_1$, we predict that the phase shift depends inversely on the window size and inversely on the one-third power of velocity, $\Phi_0 \propto w^{-1}v^{-1/3}$, whereas one might naively have predicted that Φ_0 would depend on w^{-3} . We emphasize that this prediction assumes that the atomic wave function extends uniformly over the entire grating window, which does not apply for localized distributions of atoms in a larger cavity, such as a BEC trapped near a surface.

From eq. (8), it is apparent that an accurate C_3 is highly dependent on good knowledge of the grating geometrical parameters (d_G , w_G , L_G and α_G). These parameters were determined using the method described in [36] and we thus get the fitted value $C_3 = 3.25 \pm 0.2 \text{ meV} \cdot \text{nm}^3$. Using equation 2.36 of reference [41], we have calculated the following C_3 values: $C_3 \approx 3.10 \text{ meV} \cdot \text{nm}^3$ with the optical constants of bulk Si_3N_4 [42] and $C_3 \approx 2.95 \text{ meV} \cdot \text{nm}^3$ with the optical constants of SiN_x given in ref. [28], with the optical constants being represented, in both cases, by the Tauc-Lorentz formula [43]. The agreement is reasonably good, especially if one considers that the thin metallic Au/Pd layer should increase the C_3 coefficient.

In summary, we have been able to measure the phase shift due to the Van der Waals interaction of the atoms with a silicon nitride grating with a 2% relative uncertainty. The main impact of this research is that our improvement in precision allows us to study dispersion of this phase shift for the first time. The VdW-induced phase shift was found to scale like $v^{-0.49}$, a somewhat unusual result. We have used the observed dispersion to determine the strength and the power-law of the VdW potential. The VdW C_3 coefficient for lithium atoms and a silicon nitride surface, covered with a thin Au/Pd layer, was determined from this phase shift with 6% uncertainty. The observed dispersion is also necessary to establish a constraint on a possible non-Newtonian gravitational interaction and we get an upper limit comparable to the best published values for a range parameter $\lambda \approx 2$ nm.

We thank the technical staff of the LCAR laboratory for their precious help and high-quality work. We also thank A. LAMBRECHT for helpful advice. The Toulouse group thanks CNRS department MPPU, Région Midi-Pyrénées and ANR (grant ANR-05-BLAN-0094) for support. ADC thanks NSF for Grant No. PHY-0653623.

REFERENCES

- [1] CRONIN A. D., SCHMIEDMAYER J. and PRITCHARD D. E., *Rev. Mod. Phys.*, **81** (2009) 1051.
- [2] PERREAULT J. D. and CRONIN A. D., *Phys. Rev. Lett.*, **95** (2005) 133201.
- [3] EKSTROM C. R., SCHMIEDMAYER J., CHAPMAN M. S., HAMMOND T. D. and PRITCHARD D. E., *Phys. Rev. A*, **51** (1995) 3883.
- [4] MIFFRE A., JACQUEY M., BÜCHNER M., TRÉNEC G. and VIGUÉ J., *Phys. Rev. A*, **73** (2006) 011603(R).
- [5] DESSLER B., HUGHES K. J., BURKE J. H. T. and SACKETT C. A., *Phys. Rev. A*, **77** (2008) 031604(R).
- [6] SCHMIEDMAYER J., CHAPMAN M. S., EKSTROM C. R., HAMMOND T. D., WEHINGER S. and PRITCHARD D. E., *Phys. Rev. Lett.*, **74** (1995) 1043.
- [7] ROBERTS T. D., CRONIN A. D., KOKOROWSKI D. A. and PRITCHARD D. E., *Phys. Rev. Lett.*, **89** (2002) 200406.
- [8] JACQUEY M., BÜCHNER M., TRÉNEC G. and VIGUÉ J., *Phys. Rev. Lett.*, **98** (2007) 240405.
- [9] CASIMIR H. B. G. and POLDER D., *Phys. Rev.*, **73** (1948) 360.
- [10] <http://www.cfa.harvard.edu/~babb/casimir-bib.html>.
- [11] GRISENTI R. E., SCHÖLLKOPF W., TOENNIES J. P., HEGERFELDT G. C. and KÖHLER T., *Phys. Rev. Lett.*, **83** (1999) 1755.
- [12] GRISENTI R. E., SCHÖLLKOPF W., TOENNIES J. P., HEGERFELDT G. C., KÖHLER T. and STOLL M., *Phys. Rev. Lett.*, **85** (2000) 2284.
- [13] BOUSTIMI M., BAUDON J., DUCLOY M., REINHARDT J., PERALES F., MAINOS C., BOCVARSKI V. and ROBERT J., *Eur. Phys. J. D*, **17** (2001) 141.
- [14] BREZGER B., HACKERMÜLLER L., UTENTHALER S., PETSCHINKA J., ARNDT M. and ZEILINGER A., *Phys. Rev. Lett.*, **88** (2002) 100404.
- [15] LANDRAGIN A., COURTOIS J.-Y., LABEYRIE G., VANSTEENKISTE N., WESTBROOK C. I. and ASPECT A., *Phys. Rev. Lett.*, **77** (1996) 1464.
- [16] WESTBROOK N., WESTBROOK C. I., LANDRAGIN A., LABEYRIE G., COGNET L., SAVALLI V., HORVATH G., ASPECT A., HENDEL C., MOELMER K., COURTOIS J.-Y., PHILLIPS W. D., KAISER R. and BAGNATO V., *Phys. Scr.*, **T78** (1998) 7.
- [17] COGNET L., SAVALLI V., HORVATH G. Zs. K., HOLLEVILLE D., MARANI R., WESTBROOK N., WESTBROOK C. I. and ASPECT A., *Phys. Rev. Lett.*, **81** (1998) 5044.
- [18] SZRIFTGISER P., GURY-ODELIN D., ARNDT M. and DALIBARD J., *Phys. Rev. Lett.*, **77** (1996) 4.
- [19] GORLICKI M., FERON S., LORENT V. and DUCLOY M., *Phys. Rev. A*, **61** (1999) 013603.
- [20] SHIMIZU F. and FUJITA J., *Phys. Rev. Lett.*, **88** (2002) 123201.
- [21] GRUCKER J., KARAM J.-C., CORREIA F., PERALES F., VASSILEV G., BOCVARSKI V., CHÉRIF S. M., BAUDON J. and DUCLOY M., *Eur. Phys. J. D*, **41** (2007) 467.
- [22] GRUCKER J., BAUDON J., PERALES F., DUTIER G., BOCVARSKI V., KARAM J.-C., VASSILEV G. and DUCLOY M., *Eur. Phys. J. D*, **47** (2008) 427.
- [23] ZHAO B. S., SCHULZ S. A., MEEK S. A., MEIJER G. and SCHÖLLKOPF W., *Phys. Rev. A*, **78** (2008) 010902.
- [24] LIN Y. J., TEPER I., CHIN C. and VULETIĆ V., *Phys. Rev. Lett.*, **92** (2004) 050404.
- [25] SAGUE G., VETSCH E., ALT W., MESCHÉDE D. and RAUSCHENBEUTEL A., *Phys. Rev. Lett.*, **99** (2007) 163602.
- [26] HARBER D. M., OBRECHT J. M., MCGUIRK J. M. and CORNELL E. A., *Phys. Rev. A*, **72** (2005) 033610.
- [27] DIMOPOULOS S. and GERACI A. A., *Phys. Rev. D*, **68** (2003) 124021.
- [28] BRÜHL R., FOUQUET R. P., GRISENTI R. E., TOENNIES J. P., HEGERFELDT G. C., KÖHLER T., STOLL M. and WALTER C., *Europhys. Lett.*, **59** (2002) 357.
- [29] PERREAULT J. D., CRONIN A. D. and SAVAS T. A., *Phys. Rev. A*, **71** (2005) 053612.
- [30] PERREAULT J. D. and CRONIN A. D., *Phys. Rev. A*, **73** (2006) 033610.
- [31] DRUZHININA V. and DEKIEVIET M., *Phys. Rev. Lett.*, **91** (2003) 193202.
- [32] BLOCH D. and DUCLOY M., *Adv. At. Mol. Opt. Phys.*, **50** (2005) 91.
- [33] HOINKES H., *Rev. Mod. Phys.*, **52** (1980) 933.
- [34] MCGUIRK J. M., HARBER D. M., OBRECHT J. M. and CORNELL E. A., *Phys. Rev. A*, **69** (2004) 062905.
- [35] MIFFRE A., JACQUEY M., BÜCHNER M., TRÉNEC G. and VIGUÉ J., *Eur. Phys. J. D*, **33** (2005) 99.
- [36] LONIJ V. P. A., HOLMGREN W. F. and CRONIN A. D., submitted to *Phys. Rev. A* (2009) <http://arxiv.org/abs/0904.3289v1>.
- [37] PERREAULT J. D. and CRONIN A. D., *J. Phys.: Conf. Ser.*, **19** (2005) 146.
- [38] CRONIN A. D. and PERREAULT J. D., *Phys. Rev. A*, **70** (2004) 043607.
- [39] BORDAG M., MOSTEPANENKO V. M. and SOKOLOV I. YU., *Phys. Lett. A*, **187** (1994) 35.
- [40] HEILMANN R. K., AHN M., GULLIKSON E. M. and SCHATTENBURG M. L., *Opt. Express*, **16** (2008) 8658.
- [41] ZAREMBA E. and KOHN W., *Phys. Rev. B*, **13** (1976) 2270.
- [42] PHILIPP H. R., in *Handbook of Optical Constants of Solids I*, edited by PALIK E. D. (Academic Press, New York) 1985, p. 771.
- [43] JELLISON G. E. jr. and MODINE F. A., *Appl. Phys. Lett.*, **69** (1996) 371; 2137.